JOURNAL OF Materials CHEMISTRY

Sol–gel synthesis and photoluminescent properties of cerium-ion doped yttrium aluminium garnet powders

Chung-Hsin Lu,* Hsin-Cheng Hong and R. Jagannathan†

Electronic and Electro-optical Ceramics Laboratory, Department of Chemical Engineering, National Taiwan University, Taipei, Taiwan, R.O.C

Received 21st January 2002, Accepted 10th April 2002
First published as an Advance Article on the web 8th May 2002

Luminescent $Y_3Al_5O_{12}:Ce^{3+}$ ($YAG:Ce^{3+}$) ceramics with nanometer- to micronmeter-sized particles were prepared by a new sol–gel pyrolysis method. Notwithstanding thermochemical considerations, the combined fuel system of urea and poly(vinyl alcohol) (PVA) yielded nanoparticles exhibiting single-crystal features. This can be attributed to the pyrolysis of sols trapped within the cages formed by the cross-linking of PVA chains in the presence of urea. Another salient feature of this investigation is the higher luminescence yield for $YAG:Ce^{3+}$ samples prepared using only urea as the fuel at much lower temperature (1000 °C) compared to $YAG:Ce^{3+}$ samples prepared by the conventional solid-state reaction method at 1450 °C. In addition, the partial aliovalent substitution of Y^{3+} by Ba^{2+} in this important luminescent ceramic results in new defect complexes serving as precursors for the generation of excitons. Under band-edge photoexcitation, the excitons thus generated can resonate with excited levels of Ce^{3+} which have a profound dependence on the particle size.

Introduction

Development of new nanophotonic materials has become a great challenge to the people working in materials research in view of their ever increasing scope for novel applications and interesting optoelectronic properties. With the advent of this new class of materials, creation of new technologies such as quantum well lasers and UV radiation blockers has become possible.[1] In particular, doped nanocrystals, besides their tremendous potential for applications, form an exciting field of materials research from a basic science point of view. In these nanocrystalline systems, more reliable information can be obtained concerning the spatially confined host–guest interactions, and local physico-chemical reactions. This is possible at the molecular level unlike macroscopic systems where these are lost owing to ensemble averaging effects. Over the last decade, for the preparation of nanocrystalline ceramic systems, several new chemical techniques such as spray-drying, freeze-drying, sol–gel, co-precipitation and self-sustaining combustion syntheses have been developed.[2–4] These methods require a high degree of sophistication and control of the various parameters involved in the preparation such as temperature, atmosphere, laser power *etc*., thereby introducing limitations on up-scaling the synthesis for commercial applications.

In this study, we report a method suitable for the large-scale synthesis of nanocrystalline $Y_3Al_5O_{12}:Ce^{3+}$ ($YAG:Ce^{3+}$) in contrast to its bulk counterpart already applied in industry.[5] One such application is in luminescence conversion light emitting diodes (LUCOLED) which are poised to revolutionize the luminescent lighting industry and may replace the conventional incandescent and discharge column type fluorescent lamps. Prototype LUCOLED models have become commercially available.[6] This novel LED based lighting system exhibits long lifetime ($\sim 10^5$ h), compact size, and low power consumption. Generation of white light closer to daylight (correlated colour temperature, T_c, 4000–6500 K) with good colour rendition properties can be achieved with the proper combination of emissions from a semiconductor diode and Ce^{3+} doped yttrium aluminium garnet ($YAG:Ce^{3+}$) phosphor system. Yttrium aluminium garnet, YAG ($Y_3Al_5O_{12}$), in addition to its classical applications as an important optical ceramic such as host for phosphors,[7] lasers,[8] and optical windows,[9] is an ideal candidate for high temperature structural ceramics.[10]

Preparation of the YAG systems for these applications is highly demanding in terms of luminescence yield, and the defect chemistry of the refractory material. Owing to the optical isotropic nature of the YAG system, the powder densification ceramic technique is a viable alternative to single crystal growth.[11] Conventionally, the $YAG:Ce^{3+}$ phosphor system is prepared by a solid state reaction running to several hours/days at very high temperatures (~ 1600 °C).[12] This is a serious limitation for the production of this phosphor on an industrial scale. In addition, the particle size is another critical factor that determines luminescent properties of this important phosphor system.[13] It is certainly advantageous to have a nanoceramic analogue of this technologically important system, in particular for the preparation of thin films with minimum scattering losses so as to be compatible with LEDs for lighting applications. In order to address these issues, in this investigation we have prepared the nanocrystalline analogue of this important phosphor system by a more facile synthetic route. Also, we consider that a detailed investigation of the luminescent properties of nanocrystalline $YAG:Ce^{3+}$ is of practical significance. The self-propagating high temperature synthesis of phosphor materials is widely acknowledged as a method for the synthesis of micron-sized ceramic particles.[14] However, this method has the drawback of producing highly agglomerated particles. On the other hand, when this method is used along with a polymer, it is possible to produce well-dispersed nanoceramic materials. In this investigation, we employed a polymer pyrolysis method using poly(vinyl alcohol) (PVA) as the organic polymer which can serve both as the fuel for nanocrystal formation and also as a dispersing medium to limit the agglomeration of particles. Recently, there have been some reports on the synthesis of various nanoceramics employing PVA[15] and polyacrylamide (PAM)[16] in combination with other fuels.

The salient features of this facile synthesis are: no expensive precursors, large scope for tailorability with control over the size and morphology, upscalability and high relative luminescence yield. In addition, we believe that this method may

†Permanent address: Luminescence Group, CECRI (CSIR), Karaikudi-630006 (T.N.), India.

provide wider scope for large scale synthesis of various advanced nanoceramics.

Experimental procedure

Nanocrystalline $Y_3Al_5O_{12}:Ce^{3+}$ ($YAG:Ce^{3+}$) samples were prepared through a novel sol–gel pyrolysis route at relatively low temperatures around 1000–1100 °C. The basic reactions among the various chemical constituents and the homogenization, heat-treatment steps, are as indicated in Eqn. (1).

$$\begin{aligned} &YNO_3\ (0.1425\ M)+CeNO_3\ (0.0075\ M)+AlNO_3\ (0.25\ M)+\\ &(CH_2CHOH)_n\ (0.4\ M)+(NH_2)_2CO\ (0.4\ M)\\ &\xrightarrow{\text{homogenization at 100°C for 2 h}}\text{sol}\xrightarrow{\text{heating at 250°C for 2 h}}\\ &\text{yellow gel}\xrightarrow{\text{calcining at 800–1100°C for 4 h}} \qquad (1)\\ &\text{phase pure nano/micro}YAG:Ce^{3+}\\ &\text{(yellow powder)} \end{aligned}$$

The chemicals, namely, YNO_3 (0.784 g), $CeNO_3$ (0.065 g), $AlNO_3$ (2.062 g), PVA (0.352 g) and $(NH_2)_2CO$ (0.480 g), were dissolved in 20 ml distilled water. The concentration of Ce^{3+} with respect to Y^{3+} was optimized at 5 mol%. Here both urea and PVA can serve as fuels. Hence three different samples were prepared by the pyrolysis method using as fuels both urea and PVA (sample I), urea only (sample II), and PVA only (sample III). The relative concentrations of the metallic nitrates were maintained constant and the combination of these reactants is represented by 'R'. The chemical compositions of reactants and the fuels used for various samples are given in Table 1. In all these cases, the molar ratio between the oxidizer (metallic nitrates) and the organic fuels was adjusted so that the ratio Φ between the sum of the oxidizing valencies to the sum of the reducing valencies in the reaction was close to unity (Table 1). These samples were compared with a $YAG:Ce^{3+}$ sample prepared by the conventional solid state reaction at 1450 °C and 6 h (Sample IV). Further, in order to study the effect of Ba^{2+} doping, three more samples, namely, I-Ba, II-Ba, III-Ba were prepared in the same way described above by substituting Ba^{2+} (10 mol%) in place of Y^{3+}

The chemical purity of the products was examined using X-ray powder diffraction (XRD) analysis at room temperature using a MAC Science MXP3 X-ray diffraction system with CuK_α radiation. The particle size, morphology and the selected area electron diffraction (SAED) pattern of the nanocrystalline sample (sample I) were analyzed using a Hitachi H-7100 transmission electron microscope (TEM) operated at 75 kV. The other samples (samples II, III and IV) were analyzed using a Hitachi S-800 scanning electron microscope. The photoluminescence spectra were recorded using a Hitachi 4500 fluorescence spectrophotometer employing a Hamamatsu R928F photo-mulitplier as the light detector, gratings with a groove density of 1200 lines mm^{-1} and a 150 W Xe arc discharge lamp as the excitation source. The excitation spectra were corrected for the beam intensity variation of the Xe light source used. Diffuse reflectance spectra were recorded using a Hitachi U3410 UV-visible spectrophotometer with optical quality $BaSO_4$ powder as the reference.

3. Results and discussion

3.1. Sol–gel pyrolysis and particle growth

The preparation of luminescent $YAG:Ce^{3+}$ is based on pyrolysing the mixture of the corresponding metallic nitrates acting as reactants and a polymeric gel base acting as a dispersing medium in the presence of a suitable fuel by a self-sustained combustion process. The effective total valency ratio, Φ, between the oxidizer (due to metallic nitrates) and fuels (urea and/or PVA) is very critical in determining the sustainability of the combustion reaction and hence obtaining the desired monophasic product. This can be given by the following equation[17]

$$\Phi=\sum x_i M_i n_i/(-1)\sum x_j F_j n_j \qquad (2)$$

where Φ is the ratio between the sum of the oxidizing valencies to the sum of reducing valencies in the reaction, while M_i and F_j are the number of ions in oxidizers and fuels respectively, x_i and x_j are the corresponding number of units in oxidizers and fuels respectively, and n is the corresponding valence for each species. When the ratio Φ is 1, maximum energy will be released for the combustion reaction to achieve the target material. At an optimum concentration of fuels and oxidizing metallic nitrates, the exothermic reaction, initiated at much lower temperatures (500–1000 °C), is expected to produce temperatures as high as 1600 °C and above.[12] The temperature generated by the combustion reaction is sufficient to produce well crystallized target phases such as YAG. The products thus obtained were well dispersed ultrafine crystalline particles having a large surface area.

The flame temperature realized during the combustion reaction is very critical in determining the phase formation and particle size given by[18]

$$T_f=T_0+(\Delta H_r-\Delta H_p)/C_p \qquad (3)$$

where T_f is the flame temperature, T_0 is the starting temperature of the reaction, ΔH_r and ΔH_p are the formation enthalpies of the reactants and the products respectively, and C_p is the heat capacity at constant pressure of the products. T_0 is considered as room temperature as the combustion reaction is started with a completely dried gel without any water content.

In this study, we employed urea, PVA and a combination of both as fuel, as given in Table 1. It is important to note that urea and PVA differ considerably in their formation enthalpies and in the moles of gases (N_2, CO_2 and H_2O) evolved during the combustion process. Hence, the formation temperature and the particle growth are influenced considerably with the change in the ratio between them. Also in all these trials, the oxidizer to fuel ratio (Φ) was maintained around 1 so that the energy released would be maximal and also completion of the reaction could be achieved. For the case of sample I prepared using the combined fuel system at an optimum value of Φ = 0.94, maximum luminescence intensity was obtained.

For calcination at lower temperatures around 800 °C, the

Table 1 Comparison of $YAG:Ce^{3+}$ particle growth under pyrolysis for various samples

Sample[a]	T(heat)/°C	T_f (cal.)/K	Φ	Mean particle size
Sample I (R + 0.4M PVA + 0.4 M urea)	1000	2146	0.94	20 nm
Sample II (R + 1.0 M urea)	1000	1607	1.0	6 μm
Sample III (R + 0.6 M PVA)	1000	2376	1.0	3 μm (also ultrafine particles ~20 nm)
Sample IV (solid state reaction)	1400	—	—	0.9 μm

[a]Reactants (R): YNO_3 (0.1425 M) + $CeNO_3$ (0.0075 M) + $AlNO_3$ (0.25 M).

nanoparticles were agglomerated and fixed in residual polymer, resembling a network-like structure with individual crystallites having an average size of 5 nm. It was possible to get well dispersed particles with larger sizes, up to 30 nm, by prolonging the heating time (4–6 h) and increasing the calcining temperature to 1100 °C. The particles have either polyhedral or dumbbell morphology depending on the calcination temperature. At lower temperatures the particles exhibit polyhedral morphology and on further heat treatment they grow in size and acquire a dumbbell morphology as reported during the preparation by other methods.[18]

Results of some important combinations of the fuel systems yielding monophasic $YAG:Ce^{3+}$ are summarized in Table 1. X-Ray diffraction (XRD) patterns obtained for all $YAG:Ce^{3+}$ samples (including Ba-doped samples) are well indexable under *Ia3d* lattice symmetry consistent with the standard ICDD file # 33-0040. The refined unit-cell parameters for various preparations are in good agreement with the standard values. The XRD patterns of samples I, II and III heated at 1000 °C are given in Fig. 1. In the case of sample II, a minor peak (indicated by *) was observed due to CeO_2 as an impurity phase. This may be due to an inhomogeneous distribution of reactants and phase-segregation in the absence of the polymeric network as dispersing medium during the combustion process. In any case, this can be ignored and Ce^{4+} (with $4f^0$ electron configuration) in CeO_2 does not show any optical transitions in the region of interest.

From the SEM photographs given in Fig. 2, a clear understanding of the particle growth and size can be obtained. Obviously, the case of PVA and urea combined fuel system seems to be significant (sample I) as this combination yielded nanosized $YAG:Ce^{3+}$ particles. Samples II and III with urea and PVA used independently as fuels yielded only micron-sized particles. Using thermochemical considerations, for the combined PVA and urea fuel system based on Eqn. (3), we estimated the highest adiabatic flame temperature (T_f) to be about 2146 K. In this case, the reaction ought to have resulted in particles with a maximum size having poly-crystalline character. But the SAED pattern (Fig. 3) obtained for sample I clearly verifies single crystal features. The spot diffraction pattern obtained for sample I suggests a 'single-crystal' nature for the crystallites. Interplanar spacing values calculated (Fig. 3) from the diffraction spots are consistent with values

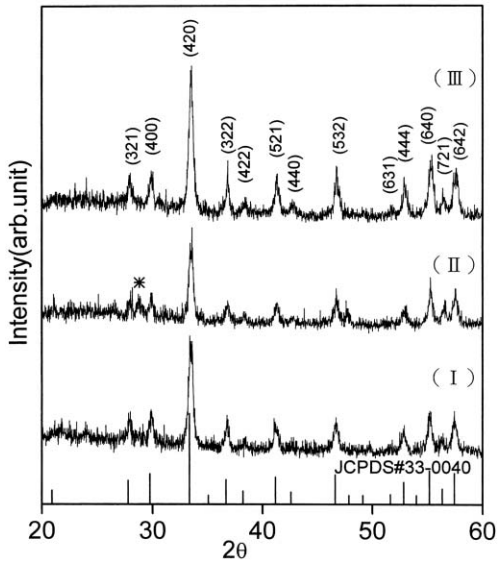

Fig. 1 X-Ray powder diffraction patterns (CuK_α radiation at T = 300 K) of $YAG:Ce^{3+}$ (5 mol%) samples prepared by sol–gel pyrolysis at 1000 °C for 4 h using (I) PVA with urea; (II) urea and (III) PVA as fuels. ICDD#33-0040 corresponding to the YAG system is also given. The weak line observed indicated by * corresponds to a CeO_2 phase.

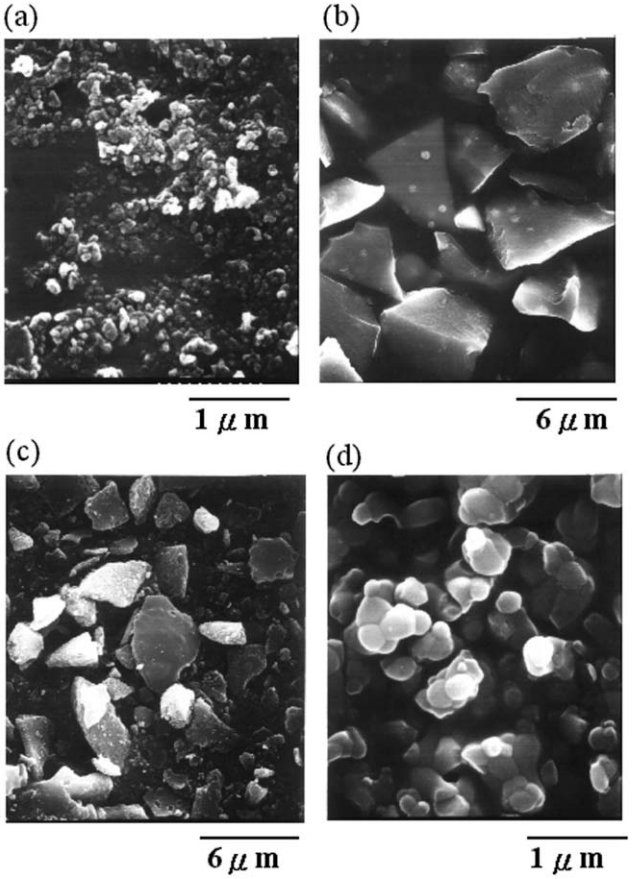

Fig. 2 Scanning electron-microscope images of $YAG:Ce^{3+}$ (5mol%) samples prepared by sol–gel pyrolysis at 1000 °C for 4 h (a) for sample I using PVA and urea; (b) for sample II using urea only and (c) for sample III using PVA only as fuels. Sample IV (d) was prepared by solid state reaction at 1450 °C for 6 h.

obtained from the standard XRD file for the YAG system (ICDD # 33-0040).

In order to account for the uniqueness of the combined fuel system, we have to consider the 'cross-linking' of the polymeric network. The linear chains of PVA can be cross-linked in the presence of urea.[19] The cross-linking between the chains may provide small cages (several nm across) wherein the 'sol' of the reactant mixture gets trapped. On thermolysis, the 'sol' trapped in the cages may be converted to ultrafine particles of $YAG:Ce^{3+}$ separately. Therefore, the cages formed by the cross-linking of PVA chains may offer resistance to the agglomeration of the particles and the particle growth.

Another interesting observation from this investigation is that unusually large particle sizes (~5 μm) are obtained for

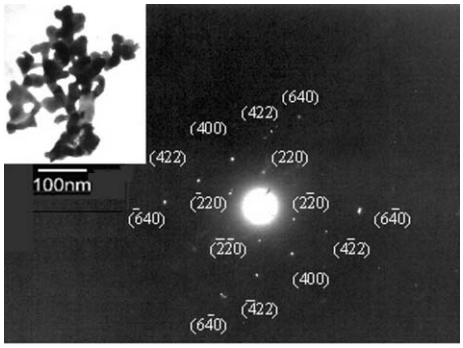

Fig. 3 Selected area electron diffraction pattern of nanocrystalline $YAG:Ce^{3+}$ (Sample I) prepared by pyrolysis at 1000 °C for 4 h using a PVA with urea fuel combination. Inset: bright-field electron microscope image of the nanocrystalline $YAG:Ce^{3+}$ sample.

samples prepared with either urea or PVA as the fuel separately. These particles are much larger than those obtained even by solid state reaction methods prepared at 1450 °C. One plausible reason may be that the flame temperature realized may be much higher than 1450 °C (Fig. 2) for these cases. This may accelerate the particle growth more than that in the solid state method. Sample III, prepared by pyrolyzing the reactants in the presence of PVA only, also had ultrafine particles (~20 nm). This can be explained by considering the cross-linking of PVA chains in the presence of water.[19]

3.2 Photoluminescence properties

Ce^{3+} with a $4f^1$ electron configuration has a ^2F_J ($J = 5/2$ and 7/2) ground state split into a doublet due to the spin–orbit interaction.[20] On photo-excitation, the 4f electron is excited to a 5d level which is further split into various Stark levels due to the crystal field exerted by the host matrix. The extent of splitting and the splitting pattern among the various Stark levels are determined by the chemical environment and the symmetry of the host matrix around a Ce^{3+} site. In the YAG system, the Y^{3+} site occupied by Ce^{3+} has distorted cubic symmetry that can be described by a rhombic D_2 point group.[21]

The emission spectra given in Fig. 4 represent the luminescence yield for various samples. From this, it can be seen that $YAG:Ce^{3+}$ sample prepared with urea only (sample II) gives a maximum yield which is about five times higher than samples I and III. From the excitation spectra (Fig. 4) corresponding to Ce^{3+} emission, the Stark-splitting pattern can be seen (hence the crystal-field values are nearly the same for all samples) and are comparable to micron-sized particles. However, for samples I and III containing nanoparticles, the spectral overlap (SO) between the emission and excitation spectra shows nearly one fold higher values when compared to samples II and IV having only micron-sized large particles. It is possible for the nanoparticles that the presence of surface states may account for the increase in the bandwidth of the emission and excitation spectra.

For sample II, the energy of maximum spectral overlap (E_{max}) is blue-shifted and is the highest when compared to the other samples, as indicated by vertical arrows in Fig. 4. This will influence the critical distance (R_c) for energy transfer between Ce^{3+} centres. The emission maxima of all the pyrolysed samples (samples I, IIand III) show a blue shift when compared with the sample IV prepared using the solid

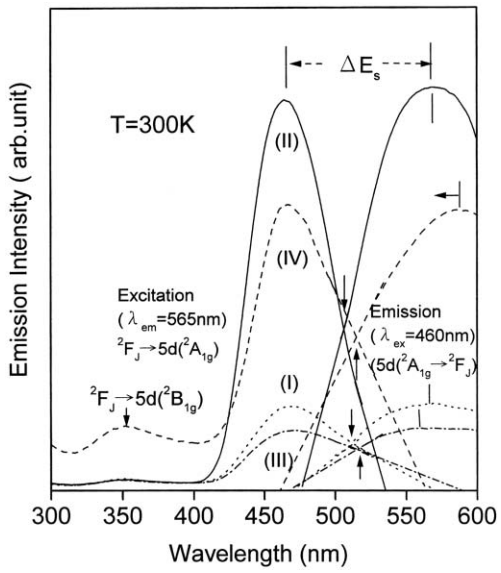

Fig. 4 Photoluminescence emission and excitation spectra of $YAG:Ce^{3+}$ (5 mol %) samples I, II, III and IV. Sample conditions are the same as those given in Fig. 2.

Table 2 Fluorescence properties of $YAG:Ce^{3+}$ samples prepared using pyrolysis

Sample	$\lambda_{emission}$/nm	$\lambda_{excitation}$/nm	ΔE_S/eV	SO/eV	E_{max}/eV	R_c/Å
I	570.8	467.8	0.48	0.47	2.42	40.02
II	568.0	464.6	0.49	0.29	2.44	36.73
III	559.0	472.0	0.41	0.53	2.41	40.95
IV	586.0	464.0	0.55	0.34	2.39	38.24

[a]ΔE_S: Stokes' shift. [b]E_{max}: energy of maximum spectral overlap. [c]R_c: critical distance for energy transfer.

state method, as indicated by a horizontal arrow. Furthermore, it is important to note that the YAG host matrix shows a complex emission band with the maximum varying between 300 and 390 nm depending on whether the sample is mono- or poly-crystalline.[22] Pronounced effects of grain boundaries and new defect centres typical of the sample conditions may well account for such a spectral-shift. Such a large variation in the emission wavelength may be attributed to a critical dependence on the oxygen stoichiometry during sample preparation. This may also influence considerably the host impurity (Ce^{3+}) energy transfer properties.

Sample III, comprising both micron- and nano-sized particles, also shows a low luminescence yield comparable to that of sample I containing only nanoparticles. The low luminescence yield in the case of nanoparticles can be attributed to pronounced non-radiative losses at grain boundaries and surface states. From Table 2, the Stokes' shift (ΔE_S) for the Ce^{3+} emission in this system shows a high value in the range of 0.4–0.5 eV. The critical distance (R_c) for energy transfer is found to be about 40 Å which is high when compared to the usual value of about 20 Å for an allowed transition. In addition, the luminescence yield of sample II, prepared by pyrolysis at 1000°C in the presence of urea, yielded about 30% higher emission intensity than sample IV, prepared by the solid state reaction at 1450 °C. This result suggests that it is possible to synthesize ceramics with a higher luminescence yield by the pyrolysis method as against the conventional solid state reaction at high temperatures and for prolonged duration.

3.3 Barium-ion substitution in the $Y_3Al_5O_{12}:Ce^{3+}$ system

For the $YAG:Ce^{3+}$ system having a low density, direct application such as scintillators in high energy radiation detection, becomes difficult. This is because the stopping power for high-energy radiation is very low for light materials. In order to overcome this, trials with the expensive lutetium (Lu) analogue have been contemplated recently.[23] However, we believe, for practical applications, partial substitution with inexpensive alternatives would be more advantageous. For this reason, we partially substituted the heavier Ba^{2+} (hence higher stopping power) for Y^{3+} and studied the resultant luminescent properties. It has been found from the XRD studies that this aliovalent substitution of Ba^{2+} in place of Y^{3+} is isostructural (Fig. 5). Nevertheless, we find substantial changes in the optical properties between Ba doped and undoped $YAG:Ce^{3+}$ samples. The aliovalent substitution of Ba^{2+} in the Y^{3+} sites of YAG is expected to produce pronounced disorder in the oxygen sublattice of the host system that can be visualized from the following Eqn. (4).

$$3(1-x)Y_2O_3 + 6xBaO + 5Al_2O_3 \rightarrow 2(Y_{1-x}Ba_x)_3Al_5O_{(12-3x/2)} \quad (4)$$

with $0 \leqslant x \leqslant 0.1$. Here oxygen vacancies ($V_O^{\bullet\bullet}$) will be formed in the above products and will act as precursors for exciton formation under band-edge photoexcitation conditions.

From Fig. 6, for the samples prepared at 1000 °C, Ba-doping showed moderate luminescence enhancement while no such enhancement was observable for the samples prepared at

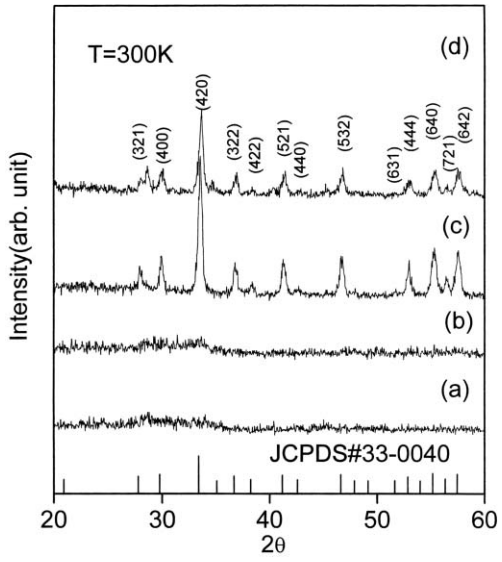

Fig. 5 X-Ray powder diffraction patterns (CuK_α radiation at T = 300 K) of YAG:Ce^{3+} (5 mol%) samples prepared by sol–gel pyrolysis using the PVA–urea combined fuel system: (a) 800 °C for 4 h without Ba^{2+}; (b) 800 °C for 4 h with Ba^{2+} (10 mol%) doping; (c) 1000 °C for 4 h without Ba^{2+} and (d) 1000 °C for 4 h with Ba^{2+} (10 mol%) doping.

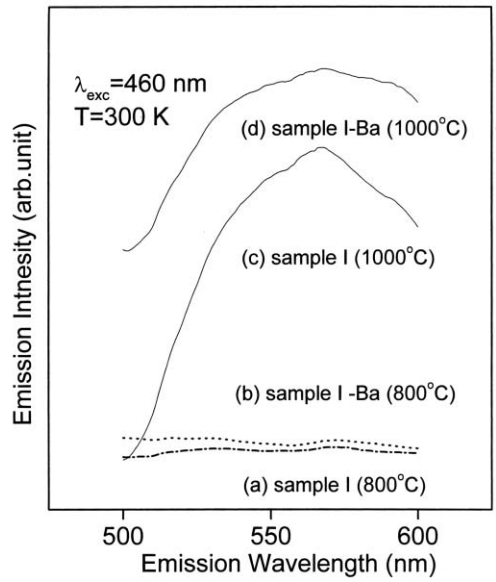

Fig. 6 Photoluminescence emission spectra of YAG:Ce^{3+} (5 mol%) samples prepared by sol–gel pyrolysis using the PVA+urea combined fuel system at (a) 800 °C for 4 h without Ba^{2+}; (b) 800 °C for 4 h with Ba^{2+} (10 mol%) doping; (c) 1000 °C for 4 h without Ba^{2+} and (d) 1000 °C for 4 h with Ba^{2+} (10 mol%) doping.

800 °C. On the other hand, diffuse reflectance spectra of samples pyrolyzed at 1000 °C did not show any measurable difference due to Ba-doping. For this reason, in Fig. 7, we present diffuse reflectance spectra of samples prepared at 800 °C only. In this context, the average particle size of all samples, irrespective of Ba-doping, depended only on the temperature, duration of the reaction and the fuel employed. Between samples II and II-Ba, prepared using only urea as the fuel, there is no difference in the diffuse reflectance spectra as a consequence of Ba-doping (Fig. 7, curves c and d). It is important to note that there are no nanoparticles in these samples. In the case of samples III and III-Ba prepared using only PVA as fuel the results obtained are just the opposite. That is, for sample III-Ba, Ba doping introduced an absorption band around 460 nm. For samples III and III-Ba, there are

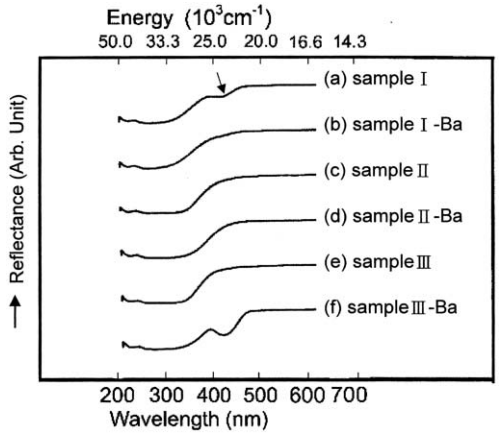

Fig. 7 Diffuse reflectance spectra of various YAG:Ce^{3+} samples prepared by pyrolysis at 800 °C for 4 h with fuels and compositions as follows: sample I without (a) and with (b) Ba^{2+} (10 mol%) doping; sample II without (c) and with (d) Ba^{2+} (10 mol%) doping; sample III without (e) and with (f) Ba^{2+} (10 mol%) doping.

nanoparticles in addition to micron-sized particles. In any case, the change in absorption features around 460 nm is observable only for the samples having nanosized particles. Further, for samples II and III prepared at 800 °C using either urea or PVA, there are large agglomerates having sizes in the range of 30–250 nm.

For samples I and I-Ba (prepared using both PVA and urea as fuels) by pyrolysis at 800 °C for 4 h, the average particle size was about 5 nm which is comparable to the exciton size. For the above two samples, unsaturated chemical bonds leading to the formation of surface states become prominent. Also the effects of the weak Ditzel ionic fields due to the aliovalent substitution[24] coupled with the creation of oxygen vacancies having a binding energy of 2.46 eV have to be considered.[25] For band-gap optical excitation, excitons generated can resonate with the various Stark levels of Ce^{3+}. In particular, the $^2A_{1g}$ and $^2B_{1g}$ Stark levels of Ce^{3+}, located at 21700 and 27700 cm^{-1} respectively in the band-gap region of the host system, can strongly overlap with the trap levels due to oxygen defects, forming exciton complexes. This is because the binding energy for the oxygen defect level is about 2.46 eV.[25] This can facilitate an intense energy transfer between the excited levels of Ce^{3+} and the exciton complexes, as illustrated in Fig. 8. When the crystallite size ($\sim$5 nm) is comparable to the exciton size, this effect is expected to be pronounced. The double-headed arrow connecting the Ce^{3+} centre (the cube) and oxygen vacancy centre (the hollow circle) by the dotted line indicates a resonance transfer process in this system.

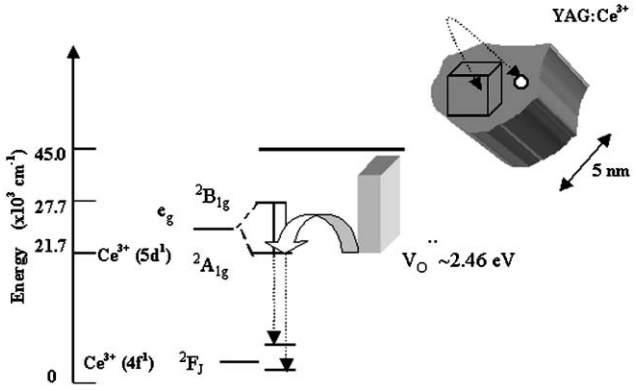

Fig. 8 A qualitative band-energy model diagram illustrating a resonance transfer between the excited Ce^{3+} level and oxygen vacancy centres acting as precursors for exciton formation due to Ba^{2+} doping in nanocrystalline YAG:Ce^{3+}.

Conclusions

A facile sol–gel pyrolysis method has been developed for the preparation of well-dispersed nanoparticles (~20 nm) of cerium-ion doped $Y_3Al_5O_{12}$ luminescent powders having potential for application in new generation luminescent lighting devices. This method, employing both poly(vinyl alcohol) (PVA) and urea as fuel and dispersing matrix, is quite suitable for scaling up the nanophosphor synthesis. The salient features of this method are a low temperature synthesis (1000 °C), nanoparticles exhibiting single-crystal like features, and a wide range of size tunability (nm to μm). The large size variation of the particles and higher luminescence yield can be achieved by varying the relative ratio of PVA to urea. The role of PVA in the synthesis for obtaining well-dispersed crystallites has also been demonstrated. An iso-structural substitution of Y^{3+} with Ba^{2+} in the $YAG:Ce^{3+}$ system suggests that the scope of this important system can be extended to high energy radiation detectors. The aliovalent substitution of Ba^{2+} leading to the generation of excitons shows some exciton–Ce^{3+} energy transfer properties having a profound dependence on particle size.

References

1 Y. Shen, C. S. Friend, Y. Jiang, D. Jakubczyk, J. Swiatkiewicz and P. N. Prasad, *J. Phys. Chem. B*, 2000, **104**, 7577.
2 W. Chang, F. Cosandey and H. Hahn, *Nanostruct. Mater.*, 1993, **2**, 29.
3 M. Kobayashi, *J. Mater. Sci. Lett.*, 1992, **11**, 767.
4 M. M. A. Sekar, S. S. Manoharan and K. C. Patil, *J. Mater. Sci. Lett.*, 1990, **9**, 1205.
5 *Phosphor Handbook*, ed. S. Shionoya and W. M. Yen, CRC Press, Washington DC, 1998, ch. 6.
6 P. Schlotter, R. Schmidt and J. Schneider, *Appl. Phys.*, 1997, **A64**, 417.
7 G. Blasse and A. Bril, *Appl. Phys. Lett.*, 1967, **11**, 53.
8 C. Greskovich and J. P. Chernoch, *J. Appl. Phys.*, 1973, **44**, 4599.
9 W. H. Rhodes, *J. Am. Ceram. Soc.*, 1981, **64**, 13.
10 T. A. Parthasarathy, T. Mah and L. E. Matson, *Ceram. Eng. Sci. Proc.*, 1990, **11**, 1628.
11 A. Ikesue and T. Kinoshita, *J. Am. Ceram. Soc.*, 1995, **78**, 1033.
12 L. E. Shea, J. McKittrick and O. A. Lopez, *J. Am. Ceram. Soc.*, 1996, **79**, 3257.
13 E. Zych, C. Brecher and H. Lingertat, *Spectrochim. Acta A*, 1998, **54**, 1771.
14 H. K. Varma, P. Mukundan, K. G. K. Warrier and A. D. Damodaran, *J. Mater. Sci. Lett.*, 1990, **9**, 377.
15 P. Pramanik, *Mater. Sci. Bull.*, 1995, **18**, 819.
16 A. Sin and P. Odier, *Adv. Mater.*, 2000, **12**, 649.
17 S. R. Jain, K. C. Adiga and V. R. Pai Verneker, *Combust. Flame*, 1981, **40**, 71.
18 M. Veith, S. Mathur, A. Kareiva, M. Jilavi, M. Zimmer and V. Zuch, *J. Mater. Chem.*, 1999, **9**, 3069.
19 *Kirk-Othmer Encyclopedia of Chemical Technology*, John Wiley and Sons, New York, 1983, vol. 23, p. 856.
20 B. G. Wybourne, *Spectroscopic Properties of Rare-Earths*, Interscience, New York, 1965.
21 D. J. Robbins, *J. Electrochem. Soc.*, 1979, **126**, 1550.
22 E. Zych, C. Brecher and H. Lingertat, *J. Lumin.*, 1998, **78**, 121.
23 E. Zych, C. Brecher, A. J. Wojtowicz and H. Lingertat, *J. Lumin.*, 1997, **75**, 193.
24 F. Zatspein, V. S. Kortov and J. V. S. Shchapova, *J. Lumin.*, 1996, **65**, 355.
25 M. Kuklja, *J. Phys.: Condens. Matter*, 2000, **12**, 295.